ISSN:1984-2295

Revista Brasileira de Geografia Física

Homepage:https://periodicos.ufpe.br/revistas/rbgfe

Ecological vulnerability in landslide risk measurement in the municipality of Barra do Turvo-SP, Brazil

Ellen Felizardo Batista[1], Larissa de Brum Passini [2]

[1] Doctoral Candidate in the Graduate Program in Civil Engineering at the Federal University of Paraná (PPGEC/UFPR). Polytechnic Center, P.O. Box 19.01, ZIP Code 81531-980, Curitiba/PR, Brazil, e-mail: ellenfp@ifsp.edu.br. ORCID: https://orcid.org/0000-0003-2947-9329 (corresponding author).
[2]Professor in the Graduate Program in Civil Engineering at the Federal University of Paraná (PPGEC/UFPR). Polytechnic Center, P.O. Box 19.01, ZIP Code 81531-980, Curitiba/PR, Brazil, e-mail: larissapassini@ufpr.br. ORCID: https://orcid.org/0000-0002-8947-4602.
Artigo recebido em 28/08/2024 e aceito em 25/02/2025.

A B S T R A C T
Landslides are significant geological events that can lead to economic, physical, and human losses, as well as degradation of ecosystems and environmental services. This study proposed a methodology to assess ecological vulnerability by incorporating landscape variables and regeneration times, and applied it in a three-dimensional ecological risk model for landslides, considering susceptibility, ecological vulnerability, and population exposure. Using Remote Sensing (RS) data and Geographic Information Systems (GIS), the methodology was applied to the municipality of Barra do Turvo-SP, a region in the Serra do Mar Mountain range with a history of landslides. Results indicated that most of the territory exhibited low (45.55%) and moderate (41.96%) ecological vulnerability, with small areas showing high (11.56%) and very low/very high (0.93%) vulnerability. The risk analysis revealed 25.55% of the area with low risk, 23.01% moderate, and 20.15% high, with the other 31.29% representing very low and very high classes. It is concluded that the proposed methodology is effective and applicable in similar contexts, highlighting the importance of conservation policies to mitigate risks and protect ecosystems. The approach, integrating ecological variables and RS and GIS data, provides a valuable tool for decision-makers in disaster prevention and environmental planning.
Keywords: Ecological values, susceptibility, remote sensing, Geographic Information Systems (GIS), three-dimensional model.

Vulnerabilidade ecológica na mensuração de risco à deslizamentos de terra no município de Barra do Turvo-SP, Brasil

R E S U M O
Deslizamentos de terra são eventos geológicos de grande impacto, resultando em perdas econômicas, físicas, humanas e na degradação de ecossistemas e serviços ambientais. Este estudo propôs uma metodologia para avaliar a vulnerabilidade ecológica, incorporando variáveis da paisagem e tempos de regeneração, e aplicá-la em um modelo tridimensional de risco ecológico de deslizamentos, considerando suscetibilidade, vulnerabilidade ecológica e exposição populacional. Utilizando dados de Sensoriamento Remoto (SR) e Sistemas de Informações Geográficas (SIG), a metodologia foi aplicada em Barra do Turvo-SP, uma região da Serra do Mar com histórico de deslizamentos. Os resultados apontaram que a maior parte do território possui vulnerabilidade ecológica baixa (45,55%) e moderada (41,96%), com pequenas áreas de alta (11,56%) e muito baixa/muito alta (0.96%). A análise de risco revelou 25,55% de risco baixo, 23,01% moderado e 20,15% alto, sendo os outros 31.29% representando as classes de risco muito baixa e muito alta. Conclui-se que a metodologia é eficaz e aplicável em contextos semelhantes, destacando a importância de políticas de conservação para mitigar riscos e proteger ecossistemas. A abordagem, integrando variáveis ecológicas e dados de SR e SIG, fornece uma ferramenta valiosa para gestores na prevenção de desastres e planejamento ambiental.
Palavras-chave: Valores ecológicos, suscetibilidade, sensoriamento remoto, Sistemas de Informação Geográfica (SIG), modelo tridimensional.

Introduction

In recent years, geological disasters have frequently occurred worldwide (Wan et al., 2021), causing continuous destruction of ecological environments and properties, as well as threatening human lives (Ma & Mei, 2021). In Brazil, according to the Brazilian Disaster Atlas, between 2013 and 2023, landslides were highlighted as one of the main types of geological disasters. During this period, 980 landslide occurrences were recorded (Brasil, 2023). Comprehensive analyses of the consequences of these landslides are crucial for mitigating their harmful effects (Spegel & Ek, 2022) and for the sustainable development of areas susceptible to landslides (Nanehkaran et al., 2023). A healthy ecological system is essential for species diversity and the sustainability of natural resources. However, geological disasters, such as landslides, can cause significant environmental changes. These events can lead to habitat fragmentation, changes in landscape ecology, soil erosion, and biodiversity loss, critically impacting regional ecosystems (Zhang et al., 2017).

Given these impacts, it is important to consider the concept of ecological risk. The ecological risk is the combination of (i) hazard, defined as the probability or susceptibility of a dangerous event occurring that can cause harm to the ecosystem, whether natural or human-induced; (ii) ecological vulnerability, which is the susceptibility of an ecosystem to suffer damage from external disturbances, encompassing both natural events and anthropogenic activities; and (iii) exposure, which represents the response of risk receptors to risk sources (Chen et al., 2013). Ecological risk assessment has become a popular research topic among scholars (Xu et al., 2021; Karimian et al., 2022), establishing itself as an essential area of study in global disaster prevention and mitigation strategies (Lin et al., 2021). Although ecological risk analysis is a growing field of study, much of the research has focused on events such as pollutant dispersion, floods, droughts, and typhoons (Cunha et al., 2021; Li et al., 2022). On the other hand, the assessment and specific study of ecological risk associated with geological disasters remain areas that require more attention. Despite advances in ecological risk analysis, detailed studies on ecological vulnerability related to landslides are still scarce, particularly in mountainous regions with complex geological and ecological characteristics. This knowledge gap poses a significant challenge for risk management and environmental conservation, highlighting the need for integrated approaches that consider ecological complexity for a deeper understanding of vulnerability in disaster-prone areas. (Lin et al., 2021).

The reduction or modification of the magnitude of landslides is a complex task; therefore, it is essential to prioritize the study of exposure and system vulnerabilities in the context of risk analysis (Birkmann et al., 2013). Vulnerability integrates multivariate and multidimensional attributes. There is no consensual or widely accepted definition for the term "ecological vulnerability" in literature (Jiang et al., 2018), and, according to Lange et al. (2010), this term is broad and applicable to organisms, populations, communities, ecosystems, and landscapes. Ecological vulnerability assessment is a fundamental approach to mitigating environmental degradation, strengthening ecological conservation, and supporting sustainable development (Turner et al., 2003). Analyses conducted in areas prone to landslides can provide valuable insights into ecosystem resilience and guide land use and conservation policies (Wang, 2021).

Recently, studies have deepened the understanding of the relationship between ecological vulnerability and geological disasters, with an emphasis on landslides. For instance, Arrogante-Funes et al. (2021) illustrate this approach by presenting a heuristic landslide risk model that integrates a susceptibility map generated by AutoML with a vulnerability map that considers both ecological and socioeconomic factors. Using spatial data such as remote sensing and official Mexican databases, their study, applied in the State of Guerrero, Mexico, found that the highest ecological vulnerability was located in mountainous areas. Moreover, they demonstrated that combining susceptibility and vulnerability mapping provides a valuable initial tool for addressing landslide-related disasters.

Similarly, Xiao et al. (2023) developed an ecological environment vulnerability assessment system for mountainous regions with complex topography, incorporating data on vegetation, topography, soil, meteorological, and social factors. Applied to the mountainous region of western Sichuan, China, their model indicated an overall medium vulnerability. The correlation between vulnerability and geological factors was non-linear, highlighting the influence of multiple human and natural variables. These findings provide an important scientific basis for environmental management in mountainous regions.

Additionally, Broquet et al. (2024) conducted a global-scale assessment, expanding the ecological perspective in landslide susceptibility assessments by integrating ecological factors such as the Normalized Difference Vegetation Index (NDVI) and Land Use and Land Cover (LULC), thereby fostering collaboration between disaster risk reduction and conservation efforts.

In line with these studies, the present research aims to evaluate ecological vulnerability and identify the areas and ecosystems most susceptible to negative impacts from landslides.

Assessing ecological vulnerability has significantly benefited from Remote Sensing (RS) and Geographic Information Systems (GIS) technologies, which enable the effective integration of natural, social, and economic indicators across large spatial and temporal scales. Li et al. (2021) demonstrated the effectiveness of GIS in detailed spatial heterogeneity analysis for ecological risk assessments, as evidenced by its application in the Qinling Mountains, located in north-central China, where factors such as population density and vegetation cover (NDVI) were mapped with precision. This approach highlights the importance of GIS for mapping and analyzing ecological risks at various scales, providing a solid foundation for regional ecological safety management and optimization.

Kamran and Yamamoto (2023) conducted a global-scale review of 80 studies and noted both qualitative and quantitative growth in research utilizing these technologies, emphasizing the frequent use of data sets such as Landsat and software like ArcGIS.

In this context, the application of RS and GIS techniques has proven effective for capturing data from multiple sources and providing detailed spatial analysis, and it is applied in the present research.

The central hypothesis of this research is that an integrated assessment of ecological vulnerability can identify areas and ecosystems more susceptible to negative impacts associated with landslides. This approach is particularly effective when applied in a three-dimensional model that combines landslide susceptibility and human exposure, using RS and GIS data to provide a detailed understanding of the spatial distribution of ecological risk.

The municipality of Barra do Turvo-SP, Brazil, where this methodology was applied, lacks detailed studies on the subject. This region, characterized by mountainous environments, has a history of landslides due to geological, geotechnical, and geomorphological characteristics, as well as hydrological discontinuities related to the local hot and humid climate. Anthropogenic factors such as urbanization, agriculture, and deforestation also contribute to increasing risk areas.

Therefore, the main objective of this study is to conduct a comprehensive assessment of ecological vulnerability in Barra do Turvo-SP, Brazil, incorporating landscape variables and regeneration times. Additionally, it aims to apply this assessment in a three-dimensional ecological risk analysis that considers landslide susceptibility and population exposure. The research relies on remote sensing, GIS technologies, and open-access data to provide a robust analysis that can be replicated in other regional contexts.

Materials and methods

Study area

Barra do Turvo is a municipality in the state of São Paulo, located in southeastern Brazil, and has a territorial area of 1,007,684 km² (Figure 1).

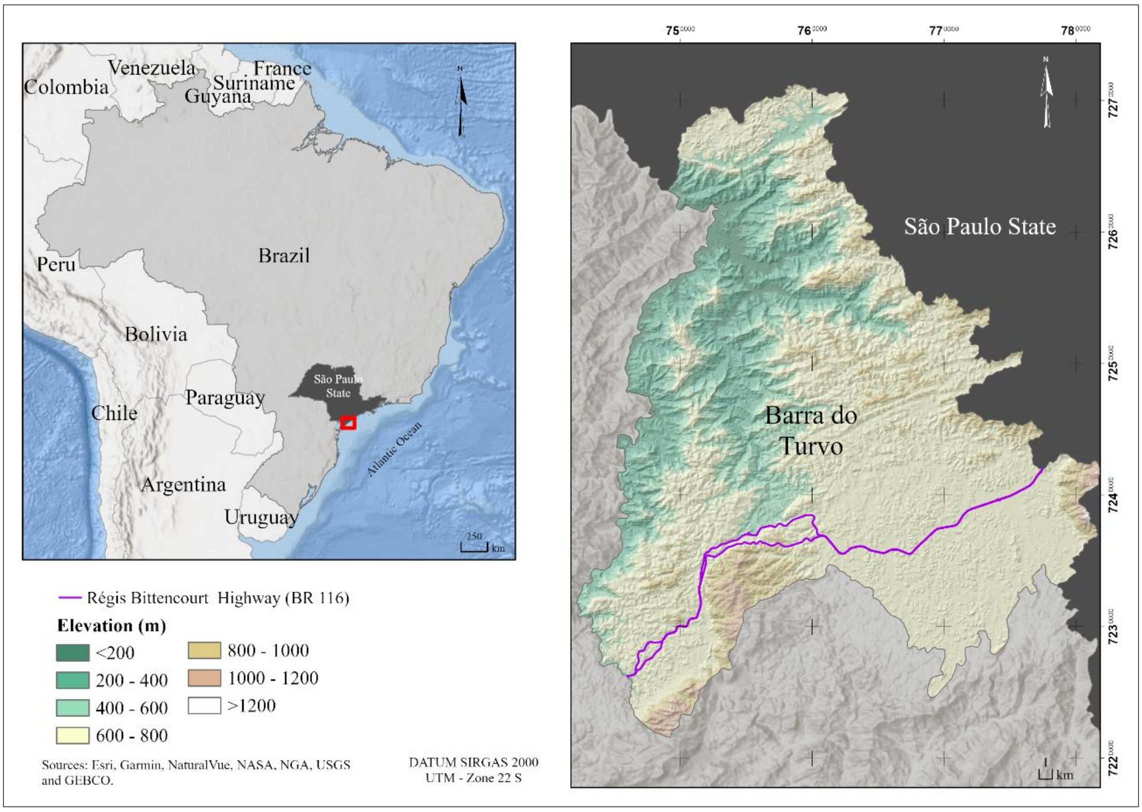

Figure 1. Location of the Barra do Turvo municipality - SP, Brazil.

The region belongs to the Serra do Mar Paranapiacaba escarpments (IBGE, 2006) and has extensive slopes and steep inclines, accompanied by deep and relatively narrow valleys. The altimetric variation is from 100 m in lower altitude areas to 1,200 m in the highest portions, with an average altitude in the range of 700 to 900 m (Ross, 2002).

Barra do Turvo's geomorphological characteristics confer an intrinsic fragility to its ecological environment. The geological composition of the region is complex (Faleiros & Pavan, 2013). The topographic characteristics, combined with the geological nature of Serra do Mar, contribute to the frequent occurrence of landslides (Cerri et al., 2018), generally in the form of shallow translational movements (Riedel, 2010). The Arteris concessionaire, which is responsible for BR-116 – a highway that crosses the municipality –, reported 93 landslide occurrences in the region from 2010 to 2018 (APRB, 2019).

According to the Köppen-Geider system, the climate is classified as humid subtropical with cool summer (Cfb) in the upper regions and humid subtropical with hot summer (Cfa) in the lower regions (SSE, 2010). The average annual precipitation varies between 1,500 and 2,000 mm, with an average annual temperature of 21.5 °C (Rousselet-Gadenne, 2004).

Regarding hydrological aspects, the region belongs to the Ribeira de Iguape drainage basin, characterized by an extensive network of tributaries of the Ribeira River. The county is located in the Atlantic Forest biome and more than 70% of its territory is in conservation units (Bim & Furlan, 2013). With 6,875 inhabitants (IBGE, 2022), concentrated mainly in rural areas, the majority of the county's population works in agriculture, livestock, and extractive exploration (Brandão et al., 1999). The region also has high levels of poverty and low life quality indicators (Coelho & Favareto, 2008).

Given the region's characteristics, such as steep slopes and other geological aspects, high rainfall index, anthropological influences on the physical environment, and past landslide occurrences, it is a region of interest for studies aimed at mitigating risks related to landslides.

Ecological risk

Ecological risk is the adverse impact that accidents or disasters can cause on the ecosystem or on its components within a given area (Lin et al., 2021). According to other relevant studies (Chuvieco et al., 2014; Zong et al., 2023), the ecological risk of a geological disaster can be defined as a three-dimensional model that considers hazard, vulnerability, and exposure. Exposure represents the response of risk recipients to risk sources; vulnerability is related to the potential damage that disasters can cause to ecosystems; and hazard represents the probability of landslide occurrence (susceptibility). Figure 2 presents a flowchart of the ecological risk assessment process in the study area.

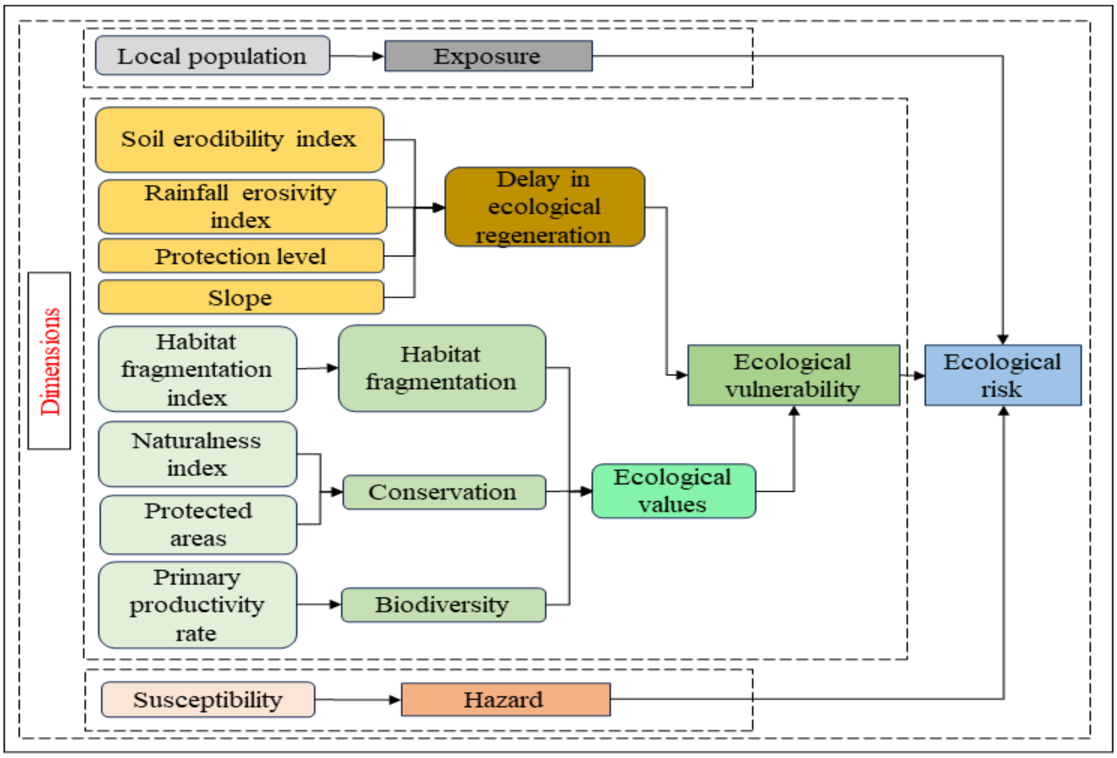

Figure 2. Flowchart of the ecological risk assessment process in the study area.

Exposure

The exposed local population was considered to be at risk after the occurrence of geological disasters, since populations are the first risk elements that require protection in a territory (Guillard-Gonçalves et al., 2014), and the interaction between human activities and natural environments can exacerbate the susceptibility of ecosystems to hazards. By incorporating human exposure into the analysis, a holistic assessment of ecological risks is provided, acknowledging the dual impact on both human and ecological systems. The mapping of the exposed population was analyzed based on the 2022 census data, as these were the only open-access data available for the study area. In the analysis, the exposed population was represented by points, with each point corresponding to 50 inhabitants, using the dot density tool in ArcGIS. The population data for each census tract were aggregated and proportionally distributed within each tract.

Ecological vulnerability

The representation of ecological vulnerability was adapted from the model proposed by Arrogante-Funes et al. (2021). The model was used in a landslide risk assessment, considering the ecological factors of the landscape - ecological values, and the delay in ecological regeneration (Figure 2). The assessment of ecological vulnerability to landslides was conducted by integrating the mapping of ecological values with the delay in ecological regeneration (Table 1).

Table 1. Ecological vulnerability to landslides resulting from ecological values and delay in ecological regeneration.

Ecological values	**Delay in ecological regeneration**				
	Very low	**Low**	**Moderate**	**High**	**Very high**
Very low	Moderate	High	High	Very high	Very high
Low	Moderate	Moderate	High	High	Very high
Moderate	Low	Moderate	Moderate	High	High
High	Low	Low	Moderate	Moderate	High
Very high	Very low	Low	Low	Moderate	Moderate

Ecological values

The ecological values were determined through the evaluation of indicators that measure the quality of ecosystems. These indicators are related to three specific aspects: biodiversity; conservation status; and habitat fragmentation. Using the ArcGIS software, the variable layers were resampled and reprojected to the same pixel size (10 x 10 m) and projection (SIRGAS 2000 UTM Zone 22S).

For the biodiversity indicator, Net Primary Production (NPP) was used as a variable to represent the amount of carbon recently fixed by photosynthesis in the plant community per unit of space and time. The total amount of carbon fixed by an ecosystem is called Gross Primary Production (GPP). Thus, NPP is the difference between GPP and the carbon consumed during plant respiration (Chapin et al., 2002). NPP stands out as a fundamental indicator of ecosystems' ecological integrity, management of natural resources, and the carbon cycle in the biosphere. Thus, it is a relevant variable for scientific research and the maintenance of environmental balance (Cao et al., 2004).

The model used to estimate NPP was made available by the USA's National Aeronautics and Space Administration (NASA) as part of the Earth Observing System (EOS) program, and it is derived from the Moderate Resolution Imaging Spectroradiometer (MODIS) sensor aboard the satellite Terra (Xiong et al., 2011). In this study, the product MOD17A3HGF - version 6.1 was used. It employs an algorithm to continuously estimate NPP in terms of space and time, on an annual basis, with a spatial resolution of 500 m (Running and Zhao, 2021). The annual NPP value for 2022 was obtained by calculating the average of all 8-day Net Photosynthesis (NPS) products from MOD17A2H. This was done by summing the NPS values from each 8 days throughout the year and then dividing by the number of 8-day periods in the year.

To estimate NPP, the MODIS team employs a range of methods and data. Initially, estimates of Fraction of Photosynthetically Active Radiation (FPAR) and Intercepted Photosynthetically Active Radiation (IPAR) are multiplied to calculate the daily Absorbed Photosynthetically Active Radiation (APAR). The daily APAR is then combined with efficiency parameters, obtained through the Biome Properties Look-Up Table (BPLUT), in order to estimate the daily GPP. The second part of the algorithm calculates the annual Maintenance Respiration (MR), also considering the effects of growth respiration. The parameters used are related to specific physical information for each type of biome, as defined in BPLUT. Additionally, daily meteorological data provided by the Global Modeling and Assimilation Office Research Site (GMAO) are incorporated. Thus, the annual MR is subtracted from the annual GPP to produce an estimate of the annual NPP.

To process the variable, NPP values were converted from digital numbers to biophysical values by multiplying the pixels of the layers by a correction factor of 0.0001. Thus, the NPP values for the year 2022 were obtained, with the unit of each pixel expressed in gC m-2 year-1. The NPP values were divided into four classes using the "natural breaks" method, and each class was reclassified into values that ranged from 0.25 to 1 (Table 2).

Table 2. Criteria used in the ecological values category.

Indicator	**Variable**	**Variation**	**Reclassification**
Biodiversity	NPP	0 - 10000 gC m^{-2} $year^{-1}$	0.25 - 0.50 - 0.70 - 1
Conservation	AP	0/1	0/1
	IN	0 - 1	0 - 0.25 - 0.50 - 0.75 -1
Habitat Fragmentation	FH	1-2	0.25 - 0.50 - 0.75 -1

For the conservation status indicator, Protected Areas (PAs) and the Naturalness Index (NI) were considered variables, since protected and natural areas commonly have higher ecological values in comparison with unprotected or artificial areas, making them more ecologically vulnerable. The final conservation status was calculated based on the average of the variables referring to the PAs and the NI.

PAs are classified as geographically delimited spaces, whose main purpose is the conservation and preservation of the natural and/or cultural resources associated with them (Medeiros, 2006). A comprehensive survey of all conservation units located in the municipality of Barra do Turvo was initially conducted, consulting the National Register of Conservation Units (CNUC) maintained by the Ministry of the Environment (MMA). This database includes all categories of protected areas in Brazil, such as Ecological Stations, Biological Reserves, National Parks, Ecological Interest, National Forests, Extractive

Reserves, Fauna Reserves, Sustainable Development Reserves, and Private Natural Heritage Reserves.

The names of each conservation unit identified were used to obtain their respective shapefiles from the World Database on Protected Areas (WDPA), made available by the UN Environment Program World Conservation Monitoring Center (UNEP-WCMC) and the International Union for Conservation of Nature (IUCN). The WDPA is updated monthly and collects information from nearly 500 sources, including contributions from governments, communities, and collaborating partners (UNEP-WCMC and IUCN, 2023). The mapping of PAs was reclassified into two categories, in which 0 corresponds to non-protected areas and 1 corresponds to PAs (Table 2).

The ecosystem's NI evaluates the degree to which a given area has not been modified or influenced by human activities (Hunter et al., 1996). The construction of the NI was based on the Landscape Mosaic (LM) model and was conducted using the GuidosToolbox (Graphical User Interface for the Description of Image Objects and their Shapes) software, provided by the Joint Research Center of the European Commission (JRC) (Vogt, 2023).

In this model, based on the classes of a land use and cover map, a generalization occurs according to the similarity in natural or semi-natural environments, agricultural areas, and urban areas. In the generated map, each pixel is classified under the composition of the types of use and coverage present in a predefined neighborhood area around it, resulting in a mosaic map of the landscape. The assignment of one of the 19 possible mosaic classes to a central pixel of the moving window is determined according to the percentage of each type of land use and cover, following a tripolar classification scheme. The values that define the landscape mosaic include absence (0%), substantial presence (10%), dominance (60%), and exclusivity (100%) of each of the three types of triangle axes (Riitters et al., 2009).

Landscape mosaic classes follow a set of specific rules: in classes with cover types making up less than 10% of the landscape, the corresponding letter is not included in the class name; classes with lowercase letters (a, u, n) in their names indicate that the corresponding type of cover (agricultural, urban, natural) covers more than 10% and less than 60% of the landscape; classes with capital letters (A, U, N) reflect that the corresponding cover type represents more than 60% but less than 100% of the landscape; classes AA, UU and NN are used to identify landscapes that contain exactly 100% of the corresponding cover type. It is also possible to aggregate the 19 mosaic classes into four landscape context classes, which distinguish regions dominated by at least 60% of one of the three generic cover types from regions that are not dominated by any cover type, called mixed landscapes (Vogt, 2023).

For the land use and cover map, the WorldCover 2021 product from the European Space Agency (ESA) was used, which consists of a global raster map generated on image recognition techniques and data from the Sentinel-1 and Sentinel-2 satellites (including radar and optical images) as inputs. WorldCover 2021 maps 11 classes of land use and cover with a resolution of 10 m (Zanaga et al., 2022). The map was reclassified into four classes, with corresponding values in bytes: 1 - Agricultural (encompassing cultivation and pasture areas); 2 - Natural (representing the forest class); 3 - Urban (covering exposed land and urbanized areas); and an additional class for missing data or bodies of water, with a value equal to 0.

The processing of the landscape mosaic occurred after the inclusion of the land use and cover map previously prepared in the GuidosToolbox software. To carry out this procedure, the following resources were accessed from the menu: Image Analysis, followed by selecting the Pattern option, and subsequently choosing the Moving Window and Landscape Mosaic options. The landscape mosaic classes were reclassified resulting in the NI, in which 0 corresponds to the most artificial types of ecosystems and 1 represents the most natural ecosystems. The specific values assigned to each class corresponded to 0.25 for the An, Un, Aun, Uan, na, un, and aun classes; 0.50 for the Na, Nu, Nau classes; 0.75 for the N class; 1 for the NN class; and 0 for the A, U, Au, Ua, au, AA, and UU classes.

As for habitat fragmentation, it is crucial to recognize its role in biodiversity loss (Farina, 2022). It can be defined as the transformation of an extensive habitat into others isolated from each other, each with a smaller surface, forming a matrix of habitats different from the original (Kurki et al., 2000).

The Morphological Spatial Pattern Analysis (MSPA) implemented by Soille and Vogt (2009) in the GuidosToolbox software was considered a variable for the habitat fragmentation indicator. The MSPA methodology involves a sequence of mathematical morphological operators designed to characterize the spatial distribution of the components of an image. This approach is based on the segmentation of objects present in the foreground of a given binary image, classifying them into seven generic categories.

To carry out MSPA processing, a land use and cover map must be prepared. In the analysis, as well as in the assessment of the conservation status, WorldCover 2021 was also used. In the preparation process, the study area was coded into 3 distinct classes: 2 for the foreground, which comprises the forest areas; 1 for the background, including the remaining land use and cover classes; and 0 for regions with missing data or bodies of water.

After the preparation, the image was inserted into the Guidos Toolbox software, and four parameters were defined:

•Foreground Connectivity (Options: 4, 8): Determines how the central pixel in a 3x3 set is connected to its adjacent neighboring pixels. It can have either a shared pixel edge and pixel corner (connectivity 8) or just a shared pixel edge (connectivity 4);

•Edge Width (Options: 1, 2, 3, 4, ...): Defines the width or thickness of classes that do not correspond to the forest "core" area, meaning areas that are not part of the interior habitat;

•Transition (Options: 0, 1): Refers to the transition pixels, which are those on an edge or perforation where the core habitat area intersects with a loop or bridge. If the transition is set to 0 (to not show transition pixels), then perforations and edges will be presented as closed boundaries delimiting interior habitat areas. The program's default setting is to display transition pixels (value 1) to illustrate the detected connections;

•Intext (Options: 0, 1): Separates internal and external features, where internal features are defined as being surrounded by a perforation, such as a forest clearing, limited by the clearing's edge.

For each parameter, the program's default value was selected: 8 for Foreground Connectivity, 1 for Edge Width, 1 for Transition, and 1 for Intext. After setting the configuration parameters, the MSPA calculation was performed by accessing the menu "Image Analysis" > "Pattern" > "MSPA".

As a result of image segmentation, seven classes of patterns were generated for the foreground, composed of Core, Islet, Perforation, Edge, Loop, Bridge, and Branch. Based on the MSPA classes, a Habitat Fragmentation (HF) index was developed by assigning weights to each class, considering its potential impact on biodiversity conservation. The classes Core, Background, and Islet were evaluated with weights of 2, 1, and 1.1, respectively. Branch and Loop shared a weight of 1.2, while Perforation and Edge were assigned a weight of 1.3, and the Bridge class received a weight of 1.5. Greater weights were assigned to less fragmented areas, specifically the central zones and those related to forest patches. The assigned values were designated in accordance with conclusions from previous studies, which indicated close relationships between the resilience of an ecosystem (its ability to recover from disturbances) and its spatial coherence (the consistency or pattern of the ecosystem elements' spatial arrangement) (Opdam et al., 2006; Chuvieco et al., 2014).

HF was reclassified, with values ranging from 0.25 to 1, following the same approach as the other ecological indicators (Table 2). The final ecological value was obtained by averaging the indicators of biodiversity, conservation status, and habitat fragmentation; and categorized into four classes, ranging from 0 to 1, representing the categories of low, medium, high, and very high ecological value.

Delay in ecological regeneration

Ecological values must be correlated with different ecosystems' ability to resist landslides and regenerate after they occur, since potential damage is more intense or lasting in less resilient areas. In this study, erosion potential, which is related to soil degradation susceptibility, was considered in the analysis of ecological regeneration, as areas with this characteristic can experience a longer delay in ecological regeneration post-landslide (Thapa et al., 2024). The methodology, for Delay in ecological regeneration, was based on four elements: slope, protection level, rainfall erosivity index, and soil erodibility index.

This study employs an innovative methodology due to the integration of specific data such as FABDEM V1-0, WDPA, GloREDa, and the Soil Erodibility map from EMBRAPA, providing a unique perspective on the ecological vulnerability of the region. Thus, the delay in ecological regeneration was calculated by aggregating the four previously mentioned factors, using cross-tabulation (Table 3).

Table 3. Levels associated with delay in ecological regeneration.

Slope	Protection Levels	Rain erosivity index and soil erodibility index			
		Low	**Moderate**	**High**	**Very high**
Flat	Protected	Very low	Very low	Low	Low
Gentle	Protected	Very low	Low	Low	Moderate
Undulating	Protected	Low	Low	Moderate	Moderate
Strong	Protected	Low	Moderate	Moderate	High
Mountainous	Protected	Moderate	Moderate	High	High
Steep	Protected	Moderate	High	High	Very high
Flat	Not Protected	Very low	Low	Low	Moderate
Gentle	Not Protected	Low	Low	Moderate	Moderate
Undulating	Not Protected	Low	Moderate	Moderate	High
Strong	Not Protected	Moderate	Moderate	High	High
Mountainous	Not Protected	Moderate	High	High	Very high
Steep	Not Protected	High	High	Very high	Very high

FABDEM V1-0, a global Digital Elevation Model (DEM) that removed the heights of buildings and trees from DEM Copernicus GLO 30, was used for slope analysis. Evaluated and ranked among several global DEMs, according to Bielski et al. (2023), FABDEM achieved third place in a general quality ranking, also securing first place in the Digital Terrain Model category. The DEM was obtained from the University of Bristol Research Data Repository and has an approximate resolution of 30 m (Hawker and Neal, 2021). The slope map was created using the tools in ArcGIS Pro: Spatial Analyst Tools > Surface > Slope. When applying these tools, the output data was selected to be in percentage inclinations. The slope map, generated by DEM processing, was categorized into six classes, according to the Soil Classification System established by the Brazilian Agricultural Research Corporation (EMBRAPA, 2013).

Regarding the level of protection, data from the mapping of both protected and non-protected areas in the study region were used. The level of protection was employed to calculate the delay in ecological regeneration, indicating the area's resilience.

To calculate the rainfall erosivity index, the Global Rainfall Erosivity Database (GloREDa) was used, provided by the European Soil Data Center (ESDAC) (Panagos et al., 2023). In the model, rainfall erosivity is evaluated through the R Factor of the Revised Universal Soil Loss Equation (RUSLE) based on an available set of global data. GloREDa compiles data from 3,625 rain gauges in 63 countries. The R factor values are calculated from precipitation data with different temporal resolutions, which are normalized to 30-minute temporal resolutions using linear regression functions. The temporal coverage spans a period of 30 to 40 years, with a predominance in the years 2000 to 2010, and 1 km of spatial resolution. The rain erosivity index was categorized into five classes based on the classification proposed by Carvalho (2008).

Regarding the soil erodibility index, the Soil Erodibility to Water Erosion map of Brazil (2020), developed by EMBRAPA (2020), was used. The model reflects the soil's intrinsic capacity to resist water erosion, corresponding to the K Factor of the Universal Soil Loss Equation (USLE). This factor is influenced exclusively by attributes inherent to the soil, such as particle size, structure, organic carbon content, permeability, depth, presence or absence of a compacted layer, and stoniness.

The delay in ecological regeneration represents the necessary period for pre-landslide conditions to be re-established. Therefore, the higher the delay values, the greater the vulnerability.

Hazard

Due to the availability of a previous study regarding the susceptibility to landslides in the municipality of Barra do Turvo, the map developed by Dalmas (2012), published in the GIS of the Ribeira de Iguape River and South Coast Hydrographic Basin Committee, was used (CBH-RB). This mapping is the result of the project “Survey and monitoring of risk areas in UGRH-11 and support for Civil Defense”, financed by the São Paulo State Water Resources Fund (Fundo Estadual de Recursos Hídricos do Estado de São Paulo - FEHIDRO).

The landslide susceptibility map was prepared by integrating lithological, geomorphological, pedological, and vegetation maps. A multi-criteria analysis was conducted using Weighted Linear Combination (WLC), a deterministic approach that assigns fixed weights to each variable, using the IDRISI Andes software (Eastman, 2006). The results obtained were validated with field data. Considering that the emphasis of this research is on the measurement and assessment of ecological vulnerability and its application in risk analysis, it is recommended to consult the work of Dalmas (2012) for more details on the construction of the susceptibility map.

Ecological risk zones

To delimit the risk zones and carry out the analysis of the ecological landslide risk, the ecological vulnerability mapping was integrated into the susceptibility map.

Based on methodologies used in previous studies on risk analyses associated with landslides (Guillard-Gonçalves et al., 2014; Lacerda et al., 2014), a matrix (Table 4) was used to delineate ecological risk zones, highlighting the regions that simultaneously presented high ecological vulnerability and high susceptibility to landslides. In the model, ecological vulnerability and susceptibility are not weighted, that is, both have the same weight in risk areas.

Table 4. Matrix delineating risk zones.

Vulnerability	**Susceptibility**				
	Very low	**Low**	**Moderate**	**High**	**Very high**
Very low	Very low	Very low	Very low	Low	Moderate
Low	Very low	Very low	Low	Moderate	High
Moderate	Very low	Low	Moderate	High	Very high
High	Low	Moderate	High	Very high	Very high
Very high	Moderate	High	Very high	Very high	Very high

Results and discussion

Determination of ecological values

As a result of the characteristics of the ecological values' spatial distribution, the biodiversity indicator showed a predominance of approximately 85% of "high productivity" throughout the territory of Barra do Turvo. This is explained by the extensive Atlantic Forest coverage in the region, which aligns with the study by Silva et al. (2023), who also identified high levels of Net Primary Production (NPP) in similar tropical forest ecosystems. Pasture areas and urbanized areas accounted for the other 15% and presented lower NPP values. Throughout the municipality, NPP values ranged from 1023.15 gC m^{-2} $year^{-1}$ to 3276.20 gC m^{-2} $year^{-1}$ (Figure 3-A). NPP was considered as a variable for the biodiversity indicator, as it reflects the potential richness of species in a given region. Areas with higher NPP generally have more abundant resources to support animal and plant life (Duro et al., 2007). Consequently, this greater biological wealth increases ecological values and makes the region less vulnerable, highlighting the need for sustainable management practices and prevention measures, thus preserving the integrity of the local ecosystem.

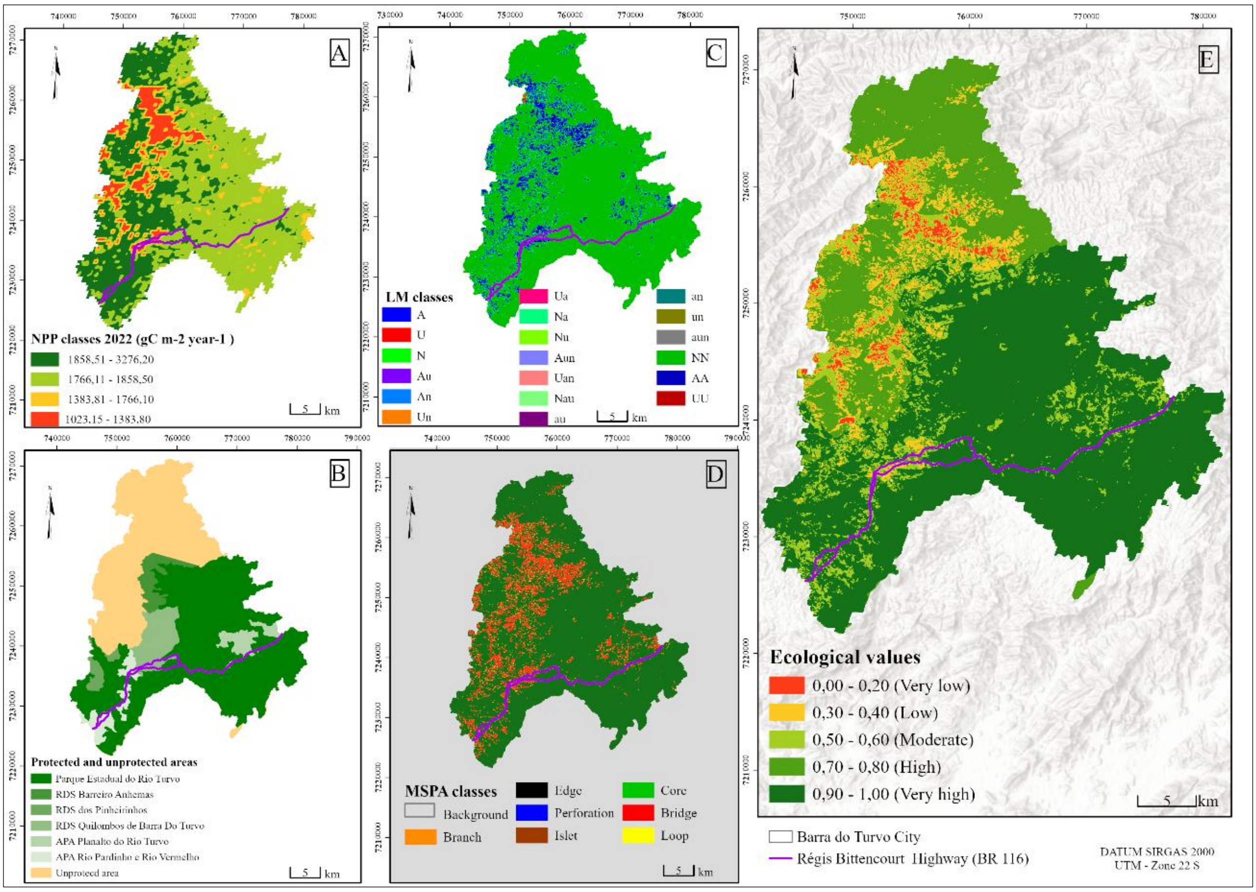

Figure 3. Spatial distribution of indicators for assessing the ecological values of the study area.

With regard to the state of conservation (Figure 3-B), 67% of the municipality's area is covered by Protected Areas (PAs), while the remaining 33% consists of non-protected areas. This significant coverage underscores the vital role of environmental preservation in maintaining the ecological stability of Barra do Turvo, contributing directly to the conservation of local ecosystems. McNeely (2020) emphasizes that PAs coverage positively influences biodiversity conservation, especially in high-value ecological areas, reinforcing the relevance of these findings.

In relation to the Naturalness Index (NI) (Figure 3-C), grouping the 19 classes of the landscape mosaic into 4 categories indicates that 86.4% of the areas correspond to natural landscapes, 10.2% to agricultural areas, 0.1% to urban areas, and 3.3% to mixed landscapes. The relatively low level of fragmentation observed may contribute to reduced ecological vulnerability and help maintain the ecological integrity of the region. The conservation status indicator plays a fundamental role in assessing the ecological values of the region, since more natural habitats are of paramount importance, not only for the protection of all layers of biological diversity but also for the preservation of essential ecosystem processes (Chuvieco et al., 2014).

As for the indicator of habitat fragmentation (Figure 3-D), in the distribution of the Morphological Spatial Pattern Analysis (MSPA) variable, 94.98% of the territory is characterized as standard Core, representing the interior habitat. The remaining 5.02% is distributed among other classes, including islet, branch, loop, edge, perforation, and bridge. The mapping of ecological values was obtained after reclassifying and calculating the average of the indicators.

The distribution of ecological values (Figure 3-E) reveals a predominance of areas classified as very high, encompassing 56.23% of the territory. High values account for 24.09%, followed by moderate values at 11.24%. Low and very low values are less common, representing

6.73% and 1.70% of the area, respectively. These results highlight the significant ecological importance of the study area, emphasizing the need to preserve these attributes in the region.

Quantifying the delay in ecological regeneration

In the analysis of the delay in ecological regeneration, regarding the slope factor (Figure 4-A), a significant presence of reliefs classified as strongly undulating (44.42%) and hilly (21.79%) was identified, together covering 66.21% of the study area. The remaining area is characterized by flat (6.17%), gently undulating (6.53%), undulating (19.49%), and steep (1.60%) terrains. The dominance of strongly undulating and hilly terrains suggests that regeneration may face challenges, especially in areas with increasing rainfall erosivity. For the level of protection, the map previously presented in Figure 3-B was used, which delimits the protected and non-protected areas of the municipality.

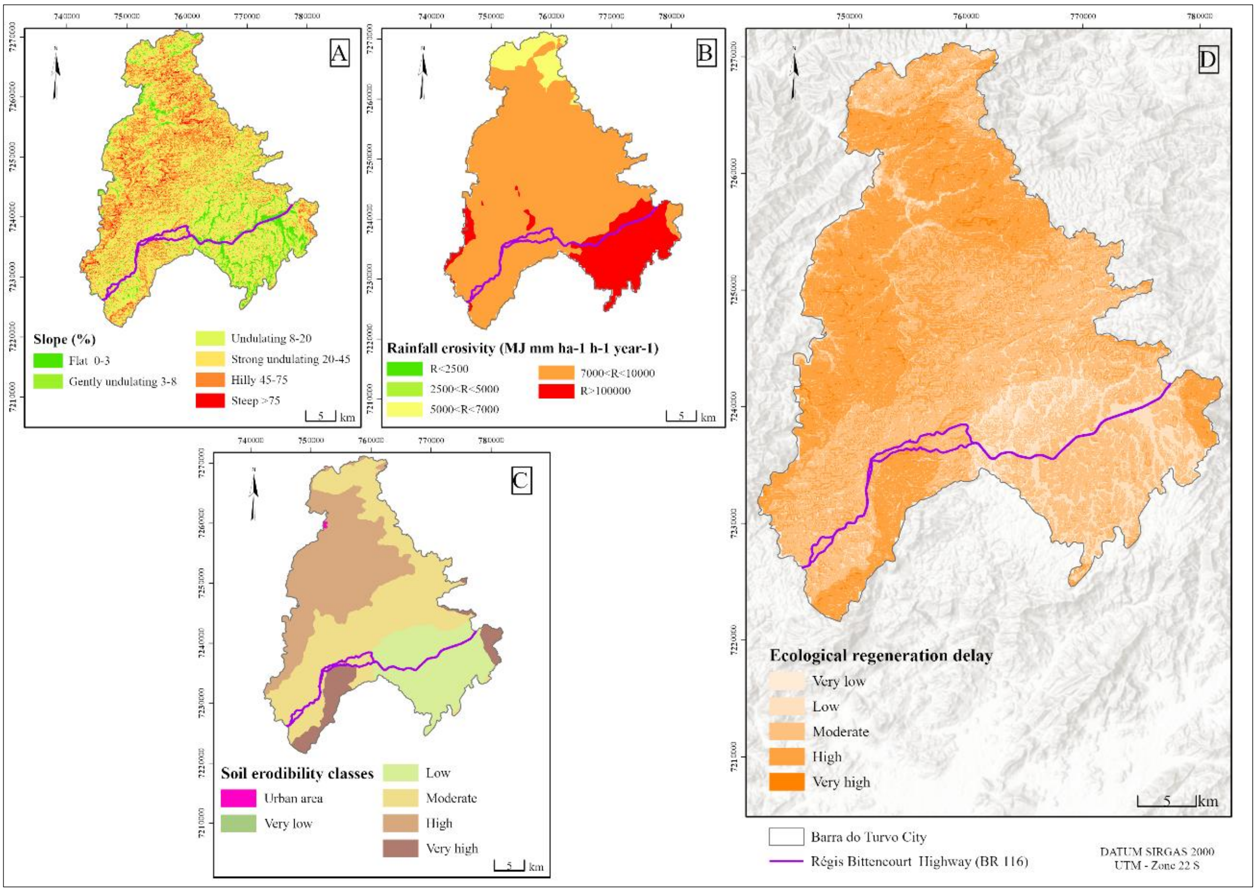

Figure 4. Spatial distribution of indicators of delay in ecological regeneration in the study area.

The variation in the rainfall erosivity index (Figure 4-B), which ranged from 6,261.78 to 11,732.30 MJ mm ha-1 h-1 year-1, highlights the potential for erosion in the region. This finding is consistent with Panagos et al. (2023), who emphasized that high rainfall erosivity plays a critical role in the erosion processes, which can further delay ecological regeneration. Spatialization indicated the absence of areas categorized as having very low and low erosivity. On the other hand, 77.14% of the municipal region had a high erosivity potential, 17.24% very high, and 5.62% moderate. Despite some uncertainties inherent to mapping using data from a global database, such as data precision and temporal variability, the results obtained are in line with previous studies, such as that of Cecílio et al. (2021), who reported erosivity index values for the municipality of Barra do Turvo ranging from 6.421 to 9.397 MJ mm ha-1 h-1 year-1, based on data from the Barra do Turvo and Rio Pardinho rainfall stations.

In relation to the soil erodibility index (Figure 4-C), which is intrinsically related to the property that makes the soil susceptible to erosion, 40.54% of the study area presents moderate levels of erosion, 31.88% high erosion, and 6.30% very high erosion. Additionally, 21.21% of the area exhibits low erosion, while 0.07% corresponds to urban areas. These findings align with observations by Stokes et al. (2014), which indicate that areas with high soil erodibility face significant challenges in maintaining ecological stability, especially following disturbances such as landslides.

After cross-tabulating the four elements referring to the delay in ecological regeneration (Figure 4-D), 47.25% of the total territorial area shows a moderate delay, 38.07% a high delay, 12.69% a low delay, 1.09% a very high delay, and 0.90% a very low delay. The delay in regeneration, associated with significant rates of erosion, suggests a fragility in the balance of the local ecosystem. The decrease in vegetation cover and soil exposure increases vulnerability, making areas prone to erosion and, consequently, landslides, especially during periods of intense rain. This situation highlights the need to implement preventive measures, such as soil conservation practices, in order to mitigate risks. Monitoring is also necessary, aiming to preserve the environment and the safety of the local community.

Ecological vulnerability assessment

The assessment of ecological vulnerability to landslides was developed by integrating the mapping of ecological values with the delay in ecological regeneration. The spatial distribution of ecological vulnerability in the study area (Figure 5-A) shows that 45.55% of the territory has low vulnerability, 41.96% has moderate vulnerability, 11.56% shows high levels of vulnerability, and 0.93% has very low/very high vulnerability.

Regions with high ecological vulnerability to landslides reflect areas where the landscape is highly fragmented, land use is intensive, ecosystem stability is threatened, and the ecology is highly fragile. In regions with low vulnerability, land development is less intense, human interference is low, and landscape fragmentation is limited.

Susceptibility mapping

The susceptibility mapping (Figure 5-B**)** indicated that 41.49% of the study area is classified as moderate, 28.29% as high, 17.13% as low, 12.42% as very high, and 0.67% as very low. In summary, 40.71% of the total area is located in regions of high and very high susceptibility to landslides.

Exposed local population

The distribution of the population in the study area (Figure 5-C) is predominantly concentrated in the urbanized regions, where higher levels of ecological vulnerability and risk are observed. In contrast, along the boundary areas, the population is more dispersed, reflecting a lower concentration in terms of both density and exposure to ecological risks. This spatial distribution highlights the significant role of urbanization in increasing vulnerability, particularly in areas with high ecological risk. The proximity of the urban areas to high-risk zones further exacerbates the potential for negative impacts on the population, especially in regions with limited resilience to ecological disturbances such as landslides.

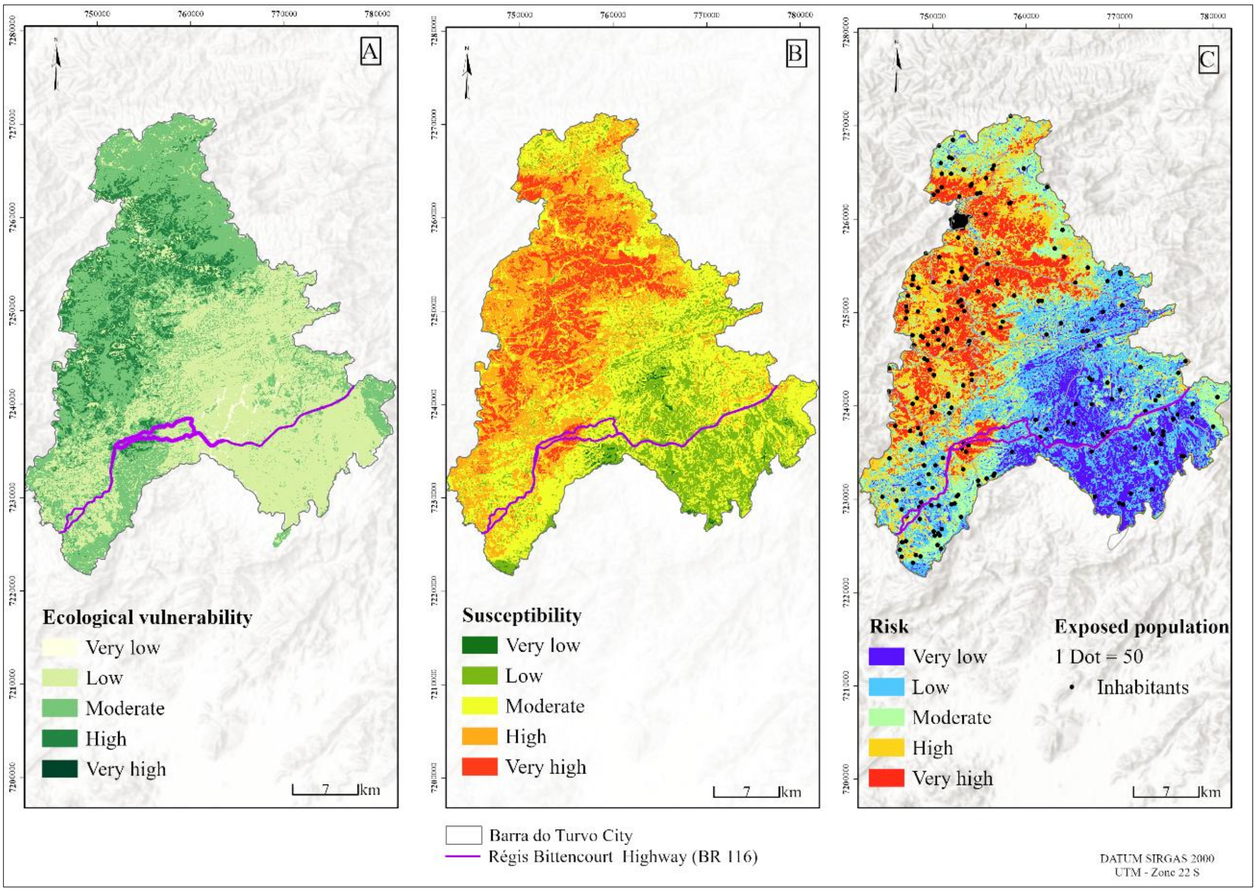

Figure 5. Spatial distribution of ecological vulnerability (a), susceptibility (b), and ecological risk zones.

Ecological risk analysis

Cross-referencing the ecological vulnerability maps (Figure 5-A) and susceptibility maps (Figure 5-B) enabled the identification of risk zones in the study area (Figure 5-C).

When examining the spatial distribution of ecological risk, it was found that 25.55% of the territory falls into low risk levels, 23.01% moderate risk, 20.15% high risk, 15.82% very high risk, and 15.47% very low risk. In other words, 35.87% of the studied region presents a risk level between high and very high.

To the northwest, areas of high risk are notably concentrated, particularly near urbanized areas, illustrating the combination of high susceptibility and ecological vulnerability. It was also observed that high-risk areas, characterized by both high vulnerability and susceptibility, tend to be concentrated in mountainous regions. In a populated area near the highway that crosses the municipality, considerable risks are present.

In the southeast region, substantially lower risk levels were identified compared to other regions, which are associated with low vulnerability and susceptibility. Additionally, some pixels in the risk map indicate circumstances in which vulnerability is high, while susceptibility is low. This can be explained by local conditions that provide resistance or mitigation to landslides, such as specific geological characteristics, the presence of resilient infrastructure, or human interventions that reduce susceptibility. The complexity of the interactions between risk factors is evident, highlighting the importance of a more detailed analysis to understand the specific dynamics of each region.

Ecological risk analysis provides a comprehensive view of the distribution of ecological risks zones, which facilitates future decisions in risk mitigation projects since more thorough efforts can be directed to areas of greater relevance.

Final considerations

The present study assessed the ecological vulnerability of the municipality of Barra do

Turvo-SP, Brazil, and applied it in an ecological risk analysis, as outlined in the initial objectives.

In order to obtain the ecological vulnerability, ecological values were considered through indicators that represent biodiversity, conservation status, and habitat fragmentation, combined with the delay in ecological regeneration, which was assessed by indicators such as slope, level of protection, index rainfall erosivity, and soil erodibility index.

The results indicated that, in relation to ecological vulnerability, 45.55% of the studied region presents low vulnerability, while 41.96% of the territory is classified as moderate vulnerability. Additionally, 11.56% of the area is categorized as high vulnerability, and 0.10% as very high vulnerability. A small portion of the region, 0.82%, falls under very low vulnerability. These findings suggest that a significant portion of the area faces moderate to low levels of ecological vulnerability, while smaller areas are more vulnerable.

In the ecological risk analysis, maps of susceptibility to landslides, ecological vulnerability, and exposure of the local population were combined. The methodology applied is pioneering in the assessment of ecological vulnerability in an area that has suffered landslides but had not been the subject of detailed investigations previously.

The specific combination of open-access data, Remote Sensing (RS) and Geographic Information Systems (GIS) techniques allows for a comprehensive view of the landscape, offering an adaptable model for other regions. Another notable characteristic is the use of open-access data, enabling accessibility and providing transparency to the process, in addition to reducing operational costs.

In terms of exposed population, the spatial distribution highlights that a significant portion of the population resides in urban areas, which are often located near zones of high ecological risk. Moreover, along the highway and in peripheral regions, a notable number of people are exposed to elevated risk levels, particularly in areas classified as high or very high risk

The ecological risk analysis showed that 25.55% of the territory presents low risk, 23.01% moderate risk, 20.15% high risk, 15.82% very high risk, and 15.47% very low risk.

So, the study area predominantly presents low vulnerability, but this does not indicate immunity to landslides. Instead, it reveals the effectiveness of the applied method in identifying areas of reduced risk. It is highlighted that, even in areas with low vulnerability, ecosystem conservation is extremely important.

The health of ecosystems is directly related to ecological risks. Healthy ecosystems have the ability to mitigate risks, contributing to the reduction of damage to ecological environments. Investing in the preservation and sustainable management of stable ecosystems is often a more effective and cost-effective strategy for disaster prevention when compared to traditional civil engineering approaches. Therefore, preserving the environment contributes to reducing the risk of landslides, which highlights the relevance of targeted approaches to environmental management

Finally, this study reinforces the need to implement effective conservation measures, ensuring not only safety but also promoting the long-term sustainability of ecosystems. The importance of further research that comprehensively addresses aspects of susceptibility, vulnerability, and exposure is also highlighted. Such studies not only improve our understanding of risks but also generate essential information to support the decisions of public managers, thus contributing to the development of more efficient strategies.

Acknowledgments

The authors would like to thank the Academic Publishing Advisory Center (*Centro de Assessoria de Publicação Acadêmica*, CAPA – http://www.capa.ufpr.br) of the Federal University of Paraná (UFPR) for assistance with English language translation and developmental editing.

References

APRB. Autopista Régis Bittencourt. (2019). Gestão da segurança dos taludes rodoviários da rodovia Régis Bittencourt, trecho da Serra do Mar PR-SP: estudos probabilísticos e monitoramento geológico-geotécnico para mensuração de riscos através de critérios econômicos. Relatório Final de Recursos de Desenvolvimento Tecnológico. Curitiba.

Arrogante-Funes, P., Bruzón, A. G., Arrogante-Funes, F., Ramos-Bernal, R. N., & Vázquez-Jiménez, R. (2021). Integration of vulnerability and hazard factors for landslide risk assessment. International journal of environmental research and public health, 18(22), 11987. https://doi.org/10.3390/ijerph182211987

Bielski, C., López-Vázquez, C., Grohmann, C. H., Guth, P. L., & Group, T. T. (2023). DEMIX Wine Contest Method ranks ALOS AW3D30, COPDEM, and FABDEM as top 1" global DEMs. arXiv preprint, arXiv:2302.08425. https://doi.org/10.48550/arXiv.2302.08425

Bim, O. J. B., Furlan, S. A. (2013). Mosaico do Jacupiranga - Vale do Ribeira / SP: conservação, conflitos e soluções socioambientais. Agrária (São Paulo. Online), 18, 4-36. https://doi.org/10.11606/issn.1808-1150.v0i18p4-36

Birkmann, J., Cardona, O. D., Carreño, M. L., Barbat, A. H., Pelling, M., Schneiderbauer, S., ... & Welle, T. (2013). Framing vulnerability, risk and societal responses: The MOVE framework. Natural Hazards, 67, 193-211. https://doi.org/10.1007/s11069-013-0558-5

Brandão, C. R., Tsikioka, C. G., & Carvalho, M. C. P. D. (1999). O cerco do verde: o olhar dos outros sobre a questão do ambiente. Ambiente & Sociedade, 2(1), 155–180. https://doi.org/10.1590/S1414-753X1999000200011

Brasil. Ministério da Integração e do Desenvolvimento Regional. Secretaria de Proteção e Defesa Civil, & Universidade Federal de Santa Catarina. Centro de Estudos e Pesquisas em Engenharia e Defesa Civil. (2023). Atlas digital de desastres no Brasil. Brasília: MIDR.

Broquet, M., Cabral, P., & Campos, F. S. (2024). What ecological factors to integrate in landslide susceptibility mapping? An exploratory review of current trends in support of eco-DRR. Progress in Disaster Science, 100328. https://doi.org/10.1016/j.pdisas.2024.100328

Cao, M., Prince, S. D., Small, J., & Goetz, S. J. (2004). Remotely sensed interannual variations and trends in terrestrial net primary productivity 1981–2000. Ecosystems, 7(3), 233–242. https://doi.org/10.1007/s10021-003-0189-x

Carvalho, N. O. (2008). Hidrossedimentologia prática. Editora Interciência.

Cecílio, R. A., de Oliveira, J. P. B., de Sousa Teixeira, D. B., Pruski, F. F., & Zanetti, S. S. (2021). Database of rainfall erosivity factor for 141 locations in Brazil. Latin American Data in Science, 1(3), 95-101. https://doi.org/10.53805/lads.v1i3.37

Cerri, R. I., Reis, F. A. G. V., Gramani, M. F., Rosolen, V., Luvizotto, G. L., Do Carmo Giordano, L., & Gabelini, B. M. (2018). Assessment of landslide occurrences in Serra do Mar Mountain range using kinematic analyses. Environmental Earth Sciences, 77, 1–16. https://doi.org/10.1007/s12665-018-7508-1

Chapin, F. S., Matson, P. A., Mooney, H. A., & Vitousek, P. M. (2002). Principles of terrestrial ecosystem ecology. Springer. New York, 1-529.

Chen, S., Chen, B., & Fath, B. D. (2013). Ecological risk assessment on the system scale: a review of state-of-the-art models and future perspectives. Ecological Modelling, 250, 25-33. https://doi.org/10.1016/j.ecolmodel.2012.10.015

Chuvieco, E., Martínez, S., Román, M.V., Hantson, S., & Pettinari, M. L. (2014). Integration of ecological and socio-economic factors to assess global vulnerability to wildfire. Global Ecology and Biogeography, 23, 2, 245-258. https://doi.org/10.1111/geb.12095.

Coelho, V. S. P., & Favareto, A. (2008). Questioning the relationship between participation and development: a case study of the Vale do Ribeira, Brazil. World Development, 36(12), 2937-2952. https://doi.org/10.1016/j.worlddev.2007.11.019

Cunha, A. C., Abreu, C. H. M., Crizanto, J. L. P., Cunha, H. F. A., Brito, A. U., & Pereira, N. N. (2021). Modeling pollutant dispersion scenarios in high vessel-traffic areas of the Lower Amazon River. Marine Pollution Bulletin, 168, 112404. https://doi.org/10.1016/j.marpolbul.2021.112404

Dalmas, F. B., Oliveira, F. R., Silva, I. S., Santos, A. J., Paranhos Filho, A. C., & Macedo, A. B. (2012). Geotechnologies on the elaboration of predictive model to identify areas susceptibility to erosion and landslides in UGRHI-11, State of São Paulo, Brazil. In Proceedings of the 34th International Geological Congress. Brisbane.

Duro, D. C., Coops, N. C., Wulder, M. A., & Han, T. (2007). Development of a large area biodiversity monitoring system driven by remote sensing. Progress in Physical Geography, 31(3), 235–260. https://doi.org/10.1177/030913330790

Eastman, R. (2006). Guide to GIS and image processing: IDRISI Andes Manual: Version 15.0. Clark Labs, Clark University.

EMBRAPA. Empresa Brasileira de Pesquisa Agropecuária. (2013). Sistema Brasileiro de classificação de solos. Centro Nacional de Pesquisa de Solos.

EMBRAPA. Empresa Brasileira de Pesquisa Agropecuária. (2020). Mapa da Erodibilidade dos Solos à Erosão Hídrica do Brasil. https://geoinfo.dados.embrapa.br/catalogue/#/dataset/2997 (Accessed August 27, 2024).

Faleiros, F., & Pavan, M. (2013). Geologia e recursos minerais da folha Eldorado Paulista SG. 22-XB-VI.

Farina, A. (2022). Principles and Methods in Landscape Ecology: An Agenda for the Second Millennium. In Principles and Methods in Landscape Ecology: An Agenda for the Second Millennium (pp. 1-42). Cham: Springer International Publishing. https://doi.org/10.1007/978-3-030-96611-9_1

Guillard-Gonçalves, C., Cutter, S. L., Emrich, C. T., & Zêzere, J. L. (2014). Application of Social Vulnerability Index (SoVI) and delineation of natural risk zones in Greater Lisbon, Portugal. Journal of Risk Research, 18(5), 651–674. https://doi.org/10.1080/13669877.2014.91068

Hawker, L., & Neal, J. (2021). FABDEM V1-0. University of Bristol.

Hunter, M., Calhoun, A. J. K., Szaro, R. C., & Johnston, D. W. (1996). A triad approach to land-use allocation, 477–491.

IBGE. Instituto Brasileiro de Geografia e Estatística. (2006). Unidades de relevo 1:5.000.000. Available at: https://www.ibge.gov.br/geociencias/informacoes-ambientais/geomorfologia/15827-unidades-de-relevo.html?=&t=acesso-ao-produto (Accessed August 27, 2024).

IBGE. Instituto Brasileiro de Geografia e Estatística. (2022). Censo 2022. https://censo2022.ibge.gov.br/panorama/ (Accessed August 27, 2024).

Jiang, Y., Shi, B., Su, G., Lu, Y., Li, Q., Meng, J., ... & Dai, L. (2018). Spatiotemporal analysis of ecological vulnerability in the Tibet Autonomous Region based on a pressure-state-response-management framework. Ecological Indicators, 130, 108054.https://doi.org/10.1016/j.ecolind.2021.108054

Kamran, M., & Yamamoto, K. (2023). Evolution and use of remote sensing in ecological vulnerability assessment: A review. Ecological Indicators, 148, 110099. https://doi.org/10.1016/j.ecolind.2023.110099

Karimian, H., Zou, W., Chen, Y., Xia, J., & Wang, Z. (2022). Landscape ecological risk assessment and driving factor analysis in Dongjiang river watershed. Chemosphere, 307, 135835. https://doi.org/10.1016/j.chemosphere.2022.135835

Kurki, S., Nikula, A., Helle, P., & Lindén, H. (2000). Landscape fragmentation and forest composition effects on grouse breeding success in boreal forests. Ecology, 81(7), 1985-1997. https://doi.org/10.1890/0012-9658(2000)081[1985:LFAFCE]2.0.CO;2

Lacerda, W. A., Palmeira, E. M., Netto, A. L. C., & Ehrlich, M. (Eds.). (2014). Extreme rainfall induced landslides: An international perspective. Oficina de Textos.

Lange, H. J. de, Sala, S., Vighi, M., & Faber, J. H. (2010). Ecological vulnerability in risk assessment - A review and perspectives. Science of the total environment, 408, 18, 3871-3879. https://doi.org/10.1016/j.scitotenv.2009.11.009

Li, C., Wang, X., Zhu, L., Liu, K., Zong, C., Wei, N., & Li, D. (2022). Enhanced impacts evaluation of Typhoon Sinlaku (2020) on atmospheric microplastics in South China Sea during the East Asian Summer Monsoon. Science of the Total Environment, 806, 150767. https://doi.org/10.1016/j.scitotenv.2021.150767

Li, X., Li, S., Zhang, Y., O'Connor, P. J., Zhang, L., & Yan, J. (2021). Landscape ecological risk assessment under multiple indicators. Land, 10 (7), 739. https://doi.org/10.3390/land10070739

Lin, J., Lin, M., Chen, W., Zhang, A., Qi, X., & Hou, H. (2021). Ecological risks of geological disasters and the patterns of the urban agglomeration in the Fujian Delta region. Ecological Indicators, 125, 107475. https://doi.org/10.1016/j.ecolind.2021.107475

Ma, Z., & Mei, G. (2021). Deep learning for geological hazards analysis: Data, models, applications, and opportunities. Earth-Science Reviews, 223, 103858. https://doi.org/10.1016/j.earscirev.2021.103858

McNeely, J. A. (2020). Today's protected areas: supporting a more sustainable future for humanity. Integrative Zoology, 15(6), 603–616. https://doi.org/10.1111/1749-4877.12451

Medeiros, R. (2006). Evolução das tipologias e categorias de áreas protegidas no Brasil. Ambiente & Sociedade, IX(1), 41-64. https://www.redalyc.org/articulo.oa?id=31709103

Nanehkaran, Y. A., Chen, B., Cemiloglu, A., Chen, J., Anwar, S., Azarafza, M., & Derakhshani, R. (2023). Riverside landslide susceptibility overview: leveraging artificial neural networks and machine learning in accordance with the

United Nations (UN) sustainable development goals. Water, 15(15), 2707. https://doi.org/10.3390/w15152707

Opdam, P., Steingröver, E., & Rooij, S. (2006). Ecological networks: A spatial concept for multi-actor planning of sustainable landscapes. Landscape and Urban Planning, 75(3-4), 322–332. https://doi.org/10.1016/j.landurbplan.2005.02.015

Panagos, P., Hengl, T., Wheeler, I., et al. (2023). Global rainfall erosivity database (GloREDa) and monthly R-factor data at 1 km spatial resolution. Data in Brief, 50, 109482. https://doi.org/10.1016/j.dib.2023.109482

Riedel, P. S., Gomes, A. R., Ferreira, M. V., Sampaio Lopes, E. S., & Sturaro, J. R. (2010). Identification of landslide scars in the region of the Serra do Mar, São Paulo State, Brazil, using digital image processing and spatial analysis tools. GIScience & Remote Sensing, 47, 498–513. https://doi.org/10.2747/1548-1603.47.4.498

Riitters, K. H., Wickham, J. D., & Wade, T. G. (2009). An indicator of forest dynamics using a shifting landscape mosaic. Ecological Indicators, 9(1), 107–117. https://doi.org/10.1016/j.ecolind.2008.02.003

Ross, J. L. S. (2002). A morfogênese da bacia do Ribeira do Iguape e os sistemas ambientais. Geousp: Espaço e Tempo (Online), 6(2), 21–46. https://doi.org/10.11606/issn.2179-0892.geousp.2002.123770

Rousselet-Gadenne, A. (2004). Étude originale Adoption d'innovations agroforestières à Barra do Turvo (São Paulo, Brésil). Cahiers Agricultures, 13, 391–402.

Running, S. W., & Zhao, M. (2021). User's Guide Daily GPP and Annual NPP (MOD17A2H/A3H) and Year-end Gap-Filled (MOD17A2HGF/A3HGF) Products NASA Earth Observing System MODIS Land Algorithm (For Collection 6) Process. DAAC. https://lpdaac.usgs.gov/documents/972/MOD17_User_Guide_V61.pdf (Accessed August 27, 2024).

Silva, L. A. P., de Souza, C. M. P., da Silva, C. R., Bolfe, É. L., & Rocha, A. M. (2023). Projection of climate change impacts on net primary productivity of the legal Amazon-Brazil. Caderno de Geografia, 33(72), 110–130. https://doi.org/10.5752/p.2318-2962.2023v33n.72p.110

Soille, P., & Vogt, P. (2009). Morphological segmentation of binary patterns. Pattern Recognition Letters, 30(4), 456–459. https://doi.org/10.1016/j.patrec.2008.10.015

Spegel, E., & Ek, K. (2022). Valuing the impacts of landslides: a choice experiment approach. Economics of Disasters and Climate Change, 6(1), 163-181. https://doi.org/10.1007/s41885-021-00101-7

SSE. Secretaria de Saneamento e Energia. (2010). Plano regional integrado de saneamento básico para UGRHI 11. São Paulo, Brasil.

Stokes, A., Douglas, G. B., Fourcaud, T., Giadrossich, F., Gillies, C., Hubble, T., ... & Walker, L. R. (2014). Ecological mitigation of hillslope instability: ten key issues facing researchers and practitioners. Plant and Soil, 377, 1–23. https://doi.org/10.1007/s11104-014-2044-6

Thapa, P. S., Daimaru, H., & Yanai, S. (2024). Analyzing vegetation recovery and erosion status after a large landslide at Mt. Hakusan, Central Japan. Ecological Engineering, 198, 107144. https://doi.org/10.1016/j.ecoleng.2023.107144

Turner, B. L., Kasperson, R. E., Matson, P. A., McCarthy, J. J., Corell, R. W., Christensen, L., ... & Schiller, A. (2003). A framework for vulnerability analysis in sustainability science. Proceedings of the national academy of sciences, 100(14), 8074-8079. https://doi.org/10.1073/pnas.1231335100

UNEP-WCMC. (2023). Protected Planet: The World Database on Protected Areas (WDPA). United Nations Environment Programme - World Conservation Monitoring Centre.

Vogt, P. (2023). User guide of GuidosToolbox: release 3.2, revision 1. European Commission, Joint Research Centre, Institute for Environment and Sustainability, Forest Resources and Climate Unit.

Wan, F., Guo, H., Li, J., Gu, M., Pan, W., & Ying, Y. (2021). A scheduling and planning method for geological disasters. Applied Soft Computing, 111, 107712. https://doi.org/10.1016/j.asoc.2021.107712

Wang, X., Zhang, C., Wang, C., Liu, G., & Wang, H. (2021). GIS-based for prediction and prevention of environmental geological disaster susceptibility: From a perspective of sustainable development. Ecotoxicology and Environmental Safety, 226, 112881. https://doi.org/10.1016/j.ecoenv.2021.112881

Xiao, H., Shao, H., Long, J., Zhang, S., He, S., & Wang, D. (2023). Spatial-temporal pattern evolution and geological influence factors analysis of ecological vulnerability in Western Sichuan mountain region. Ecological Indicators, 155, 110980. https://doi.org/10.1016/j.ecolind.2023.110980

Xiong, X., Wolfe, R., Barnes, W., Guenther, B., Vermote, E., Saleous, N., & Salomonson, V. (2011). Terra and Aqua MODIS design, radiometry, and geometry in support of land remote sensing. Land Remote Sensing and Global Environmental Change: NASA's Earth Observing System and the Science of ASTER and MODIS, 133-164. https://doi.org/10.1007/978-1-4419-6749-7_7

Xu, W., Wang, J., Zhang, M., & Li, S. (2021). Construction of landscape ecological network based on landscape ecological risk assessment in a large-scale opencast coal mine area. Journal of Cleaner Production, 286, 125523. https://doi.org/10.1016/j.jclepro.2020.125523

Zanaga, D., Van De Kerchove, R., Daems, D., De Keersmaecker, W., Brockmann, C., Kirches, G., ... & Arino, O. (2022). ESA WorldCover 10 m 2021 v200. https://doi.org/10.5281/zenodo.7254221

Zhang, F., Liu, X., Zhang, J., Wu, R., Ma, Q., & Chen, Y. (2017). Ecological vulnerability assessment based on multi-sources data and SD model in Yinma River Basin, China. Ecological Modelling, 349, 41-50. https://doi.org/10.1016/j.ecolmodel.2017.01.016

Zong, L., Zhang, M., Chen, Z., Niu, X., Chen, G., Zhang, J., Liu, H., 2023. Ecological Risk Assessment of Geological Disasters Based on Probability-Loss Framework: A Case Study of Fujian, China. International Journal of Environmental Research and Public Health, 20, 5, p. 4428. https://doi.org/10.3390/ijerph20054428.